LTR retrotransposons show low levels of unequal recombination and high rates of intraelement gene conversion in large plant genomes

Rosa Maria Cossu[a,b,1], Claudio Casola[c,1], Stefania Giacomello[d,e], Amaryllis Vidalis[f,g], Douglas G. Scofield[f,h,i,2], Andrea Zuccolo[a,j,2]

[a] Institute of Life Sciences, Scuola Superiore Sant'Anna, 56127 Pisa, Italy
[b] Department of Neuroscience and Brain Technologies, Istituto Italiano di Tecnologia (IIT), Genova, Italy
[c] Department of Ecosystem Science and Management, Texas A&M University, College Station, Texas 77843, USA
[d] Science for Life Laboratory, School of Biotechnology, Royal Institute of Technology, SE-17121 Solna, Sweden
[e] Science for Life Laboratory, Department of Biochemistry and Biophysics, Stockholm University, SE 17121 Solna, Sweden
[f] Department of Ecology and Environmental Science, Umeå University, SE-90187 Umeå, Sweden
[g] Section of Population Epigenetics and Epigenomics, Center of Life and Food Sciences Weihenstephan, Technische Universität München, 85354 Freising, Germany
[h] Department of Ecology and Genetics: Evolutionary Biology, Uppsala University, SE-75236 Uppsala, Sweden
[i] Uppsala Multidisciplinary Center for Advanced Computational Science, Uppsala University, SE-75105 Uppsala, Sweden
[j] Istituto di Genomica Applicata, Via J. Linussio 51, 33100 Udine, Italy

[1] These two authors contributed equally to this work.

[2] Corresponding authors:

DGS:
Norbyvägen 18D
SE-75236 Uppsala, Sweden
Phone: +46 18 471 64 62
email: douglas.scofield@ebc.uu.se

AZ:
Scuola Superiore Sant'Anna, Piazza Martiri della liberta' 33
56127 Pisa, Italy
Phone: +39 050 88 31 11
Fax: +39 050 88 32 35
email: a.zuccolo@sssup.it

Short title: Gene conversion, not crossing-over, at conifer TEs

Keywords: gymnosperm, *Picea*, *Pinus*, angiosperm, retroelement, gene conversion, recombination suppression, genome size

Abstract

The accumulation and removal of transposable elements (TEs) is a major driver of genome size evolution in eukaryotes. In plants, Long Terminal Repeat (LTR) retrotransposons (LTR-RTs) represent the majority of TEs and form most of the nuclear DNA in large genomes. Unequal recombination (UR) between LTRs leads to removal of intervening sequence and formation of solo-LTRs. UR is a major mechanism of LTR-RT removal in many angiosperms, but our understanding of LTR-RT-associated recombination within the large, LTR-RT-rich genomes of conifers is quite limited. We employ a novel read-based methodology to estimate the relative rates of LTR-RT-associated UR within the genomes of four conifer and seven angiosperm species. We found the lowest rates of UR in the largest genomes studied, conifers and the angiosperm maize. Recombination may also resolve as gene conversion, which does not remove sequence, so we analyzed LTR-RT-associated gene conversion events (GCEs) in Norway spruce and six angiosperms. Opposite the trend for UR, we found the highest rates of GCEs in Norway spruce and maize. Unlike previous work in angiosperms, we found no evidence that rates of UR correlate with retroelement structural features in the conifers, suggesting that another process is suppressing UR in these species. Recent results from diverse eukaryotes indicate that heterochromatin affects the resolution of recombination, by favoring gene conversion over crossing-over, similar to our observation of opposed rates of UR and GCEs. Control of LTR-RT proliferation via formation of heterochromatin would be a likely step toward large genomes in eukaryotes carrying high LTR-RT content.

Introduction

Transposable elements (TEs) are a major component of many eukaryotic genomes and long-terminal-repeat (LTR)-retrotransposons (LTR-RTs) constitute the largest part of the DNA repetitive fraction in many plants (Feschotte, et al. 2002). Because of their ability to quickly replicate and attain a very high copy number, LTR-RTs are often responsible for striking genome size variation, even between closely related species. The shrinkage of genomes via removal of LTR-RTs can also occur quickly as demonstrated in rice (Vitte, et al. 2007), maize (SanMiguel, et al. 1998), cotton (Hawkins, et al. 2009) and *Medicago truncatula* (Wang and Liu, 2008). There are two recombinant mechanisms that can remove LTR-RTs from host genomes: unequal recombination (UR), also called intrastrand homologous recombination, and illegitimate recombination (IR) (Devos, et al. 2002; Ma, et al 2004). UR occurs between LTRs of the same or different LTR-RTs and produces solo-LTRs in one step (Vicient, et al. 1999), whereas IR, which unlike UR is not homology-driven, only gradually eliminates tracts of LTR-RT sequences and leaves incomplete elements in the genome (Devos, et al. 2002; Ma, et al 2004). So far, all angiosperm genomes studied show significant frequencies of solo-LTRs (e.g., Devos, et al. 2002, Vicient, et al. 1999, SanMiguel, et al. 1996; Dubcovsky, et al. 2001; Fu and Dooner, 2002; Vitte and Panaud, 2003), thus UR is a common process in angiosperms that can counteract genome expansion via LTR-RTs. The emerging scenario in conifers is quite different: LTR-RTs seem to accumulate slowly and consistently over tens of millions of years (Nystedt, et al. 2013, Zuccolo et al. 2015), and our evidence to date suggests that the above mechanisms for LTR-RT removal have been largely inefficient (Nystedt, et al. 2013). These findings could largely explain the huge sizes characterizing many conifer genomes.

Gene conversion events (GCEs) represent another homology-driven form of recombination and, when occurring between LTRs of an LTR-RT, are another possible outcome of intraelement recombination (Chen, et al. 2007; Shi, et al. 2010). In gene conversion, a recombination event transfers DNA information from a donor sequence to an acceptor sequence, modifying the acceptor sequence without significant sequence removal (*contra* UR). Gene conversion may occur between allelic haplotypes, but GCEs that occur between LTRs of a single

LTR-RT are considered ectopic or interlocus events because they involve nonallelic sequences, similarly to the UR events that establish solo-LTRs. Although there are very few genome-wide studies on GCEs involving plant LTR-RTs, GCEs involving gene duplicates have been assessed in multiple angiosperms (Mondragon-Palomino and Gaut, 2005; Wang and Paterson, 2011; Guo, et al. 2014). About 13% of duplicated genes in rice and sorghum experienced gene conversion after separation of these lineages (Wang, et al. 2009). Physical proximity between paralogous genes facilitates gene conversion in these species (Wang and Paterson, 2011), and notably, GCEs are more common in gene-rich regions, where the density of LTR-RTs is much lower than the whole-genome average (Wang and Paterson, 2011). As would be expected for a homology-driven process, the intensity of gene conversion is also strongly associated with the sequence divergence of the loci involved, with higher divergence leading to fewer GCEs (Chen, et al. 2007; Dooner and Martinez-Ferez 1997; Li, et al. 2006).

A detailed examination of the frequency of GCEs between intraelement LTRs can also provide a more complete view of the genomic context of recombinative events involving LTR-RTs. Host genomes employ epigenetic mechanisms to suppress retroelement transcription and proliferation (Bucher, et al. 2012), and areas that are particularly rich in retroelements can condense to interstitial heterochromatin (Lippman, et al. 2004). Regions of heterochromatin, including those found at centromeres and telomeres, have long been thought to suppress homologous recombination. Recent studies contradict this assumption by indicating that it is not homology-driven repair that is suppressed within heterochromatin but rather resolution via crossing-over (Talbert and Henikoff, 2010). In maize centromeres, crossing-over is entirely suppressed but GCEs are widespread (Shi, et al. 2010), and in Drosophila, GCEs are common within centromeres and are also free of interference affecting crossing-over (Miller, et al. 2016), perhaps due to features of double-stranded break (DSB) repair specific to heterochromatin (Chiolo, et al. 2011; Peterson, 2011). Thus the fraction of genomic LTR-RTs occurring within heterochromatin could covary with relative rates of GCEs vs. UR at LTR-RTs. Further evidence for the predominant genomic context of LTR-RTs in a species could be gained by determining whether structural features of LTR-RTs are associated with UR, as has been observed in some angiosperms (Vitte and Panaud, 2003; Du, et al. 2012; El Baidouri and Panaud, 2013). Such associations could indicate that homology and other ‘local’ features of the genome can affect rates of crossing-over, while the lack of such associations could indicate that the rate of crossing-over is more strongly affected by the ‘regional’ context such as heterochromatin.

Which brings us again to the large, LTR-RT-rich genomes of conifers. To date, observations in conifers have been limited to just LTR-RT-associated UR affecting just three LTR-RT groups in a single species, Norway spruce (*Picea abies*) (Nystedt, et al. 2013). Similarly, to our knowledge, there have been few studies addressing the intensity and features of GCEs between LTR-RT elements, and none involved multiple species (Shi, et al. 2010; Kejnovsky, et al. 2007; Sharma, et al. 2013; Trombetta, et al. 2016). Here, we analyze 23 different LTR-RT groups in *P. abies* and analyze 9 LTR-RT groups in three other conifers: the closely related species white spruce (*P. glauca*) and two species belonging to the genus *Pinus* that separated from *Picea* about 140 million years ago (Buschiazzo, et al. 2012): loblolly pine (*Pinus taeda*) and sugar pine (*P. lambertiana*). We apply the same methodology to LTR-RT groups in seven angiosperm genomes: the herb *Arabidopsis thaliana*, the trees *Amborella trichopoda* and *Populus trichocarpa*, the woody vine *Vitis vinifera,* and the monocots/grasses *Brachypodium distachyon*, *Oryza sativa* (rice), and *Zea mays* (maize). The strategy we developed targeted tens of thousand of LTR-RT and solo-LTR copies at once. We also conducted a detailed analysis of rates of GCEs based upon detailed investigation of hundreds of LTR-RT elements identified in angiosperms and in *Picea abies*.

We show that the lowest rates of UR in the 11 species studied occur in the largest genomes: all four conifers as well as the angiosperm maize. We also show in our detailed analysis of GCEs that the highest rates of GCEs in the 6 species studied occur in the largest genomes, *P. abies* and maize. There is some variability in solo-LTR frequency between different LTR-RT groups in conifers, but we show in Norway spruce that this variation does not significantly correlate with any of the most evident structural features of the LTR-RT groups. Taken together, our results indicate a deep general difference in the genomic context of LTR-RTs in large, LTR-RT-rich plant genomes, and in light of other recent results, suggest that such differences may apply to eukaryotes with large genomes more generally.

Results

Using representative LTR-RTs and short reads to estimate the ratio of solo-LTRs to complete LTR-RTs

We developed the method shown in Figure 1 to infer the rate of UR by estimating the ratio of solo-LTRs to complete LTR-RTs (S-to-C ratio). Our method uses representative full-length LTR-RT sequences and short-read sequence data and determines the numbers of tracts spanning the 5' and 3' ends of the LTR that could be mapped (M) and could not be mapped (U) to the representative complete LTR-RT elements. The rationale of this approach is that genomic reads covering a complete LTR-RT should, on average, produce the same amount of mapped and unmapped tracts, whereas genomic reads covering a solo-LTR should produce only unmapped tracts. If the host genome contains only complete LTR-RT elements, then the amount of mapped versus unmapped tags should be approximately equal, resulting in an M/U ratio of ~1; due to stochastic error the ratio may occasionally slightly exceed 1. On the other hand, any notable reduction of this ratio from 1 indicates the presence of solo-LTRs in the genome (Figure 1). The ratio of solo-LTRs to complete LTR-RT elements (S-to-C) can be readily calculated as $U/M - 1$. We have extensively evaluated the consistency of the pipeline, including comparisons with results obtained via our own manual curation, evaluation of several possible biases affecting whether tracts are mapped or unmapped, establishing that relative coverage of reads datasets does not bias M/U ratios, and comparisons with previous estimates from the literature. Further details are available in Methods under 'Pipeline validation', and in supplemental tables indicated there.

We analyzed LTR-RT groups belonging to the Ty1-*copia* and Ty3-*gypsy* superfamilies in four conifer species and seven angiosperm species; sources of short-read sequence data and estimates of LTR-RT content and genome size for each studied species are provided in Table S1. See Methods for complete details of group identification and selection in the study species.

In the conifer *Picea abies*, we identified 23 abundant LTR-RT groups (7 from the Ty1-*copia* superfamily and 16 from Ty3-*gypsy*) using phylogenetic analysis (Figure S2) and applied our method to a sequence dataset containing more than 39 million 100-bp Illumina reads, corresponding to a total of 3.9 Gbp or about 0.2×

coverage of the whole genome (Table S1). For the related *P. glauca* we examined the nine most abundant of the 23 *P. abies* LTR-RT groups (5 Ty1-*copia* and 4 Ty3-*gypsy*) in a dataset of 43 million 100-bp Illumina reads (4.3 Gbp, 0.21× genomic coverage). We studied nine abundant LTR-RT groups in *Pinus taeda* (Figure S3) using 39.4 million 128-bp Illumina reads (5.04 Gbp, 0.23× coverage), and analyzed these same nine LTR-RT groups in *P. lambertiana* using a dataset of 39.4 million 128-bp Illumina reads (5.04 Gbp, 0.17× coverage) (Table S1). Representative sequences for all studied LTR-RT groups are provided in Supporting Dataset D1.

Variation in ratio of solo-LTRs to complete LTR-RTs among species

In *P. abies* we analyzed 146,028 tracts, 50,825 for Ty1-*copia* and 95,203 for Ty3-*gypsy* (Table S2A), reflecting the relative abundances of these LTR-RT superfamilies in the genome (Nystedt, et al. 2013). Assuming the read dataset is an unbiased representation of the whole genome, these figures indicate several tens of thousand elements belonging to each of these groups in the complete *P. abies* genome. The overall M/U ratio is 0.85, corresponding to an S-to-C ratio of 0.18, roughly 1 solo-LTR for every 5.6 complete LTR-RTs (Figure 2, Table S2A). In the closely related species *P. glauca* we analyzed 86,410 tracts (Table S2B). The overall M/U ratio was 0.81, with roughly 1 solo-LTR for every 4 complete LTR-RT elements (Figure 2, Table S2B). Although the underrepresentation of solo-LTRs vs. complete LTR-RT is less pronounced in *P. glauca* than in *P. abies*, the M/U ratios for the LTR-RT groups tested were not significantly different between the two *Picea* species (p = 0.21, Wilcoxon test).

In the conifer *Pinus taeda* we analyzed 153,229 tracts, yielding an overall M/U ratio of 0.88, corresponding to 1 solo-LTR to ~7.5 complete LTR-RTs (Figure 2, Table S2C). In its congener *P. lambertiana*, we analyzed 122,518 tracts (Table S2D). The overall M/U ratio was 0.79, translating to 1 solo-LTR to ~3.7 complete LTR-RTs (Figure 2, Table S2D). The M/U ratios for the LTR-RT groups studied in the two *Pinus* species did not differ significantly (p = 0.67, Wilcoxon test).

Turning to the seven studied angiosperms, we identified LTR-RT groups and applied the same method; representative LTR-RT sequences are available in Supporting Dataset D1. M/U ratios calculated for the most abundant LTR-RT groups taken as a whole are consistently lower than those calculated in conifers and S-to-C ratios are consistently higher, with the exception of *Z. mays*, which has the largest genome by far of the angiosperms studied (Figure 2, Table S3). The lowest M/U ratio among angiosperms was in *O. sativa* (0.39) and the ratios of the other analyzed species (excluding *Z. mays*) consistently indicate an excess of solo-LTRs (Figure 2, Table S3).

Previous studies in angiosperms have shown that the ratio of solo-LTRs to complete LTR-RTs is positively correlated with element features such as the LTR length (Du, et al. 2012) and the ratio of LTR length to internal region length (El Baidouri and Panaud, 2013), suggesting that, at least in angiosperms, structural features of LTR retrotransposon impact solo-LTR formation. We applied a similar analysis to the *Picea abies* dataset because it contained many more LTR-RT groups than the other three conifers. In contrast to the earlier results for angiosperms, neither of these structural features correlated with the M/U ratios of the groups (LTR length: Spearman's r_s = –0.24, p = 0.86; LTR length/internal region length: Spearman's r_s = –0.18, p = 0.8).

We extended this analysis to test two other element features, total LTR-RT abundance and LTR-RT GC content, and found no correlation between M/U ratio and either feature (element abundance: Spearman's r_s= 0.15, p = 0.76; LTR-RT GC content: Spearman's r_s = –0.05, p = 0.59).

Variation in intralement gene conversion rate among species

To identify GCEs, sequence alignments of intraelement LTRs were screened using GENECONV (Sawyer, 1999), one of the most widely used programs in gene conversion studies (e.g., Drouin, 2002; Xu, et al. 2008; Casola, et al. 2010; Casola, et al. 2012). Because of the high substitution rate experienced by TEs including LTR-RTs, the initial complete identity between converted regions of LTRs tends to be quickly eroded (SanMiguel, et al. 1998). To account for this, we combined results from several GENECONV runs at various levels of stringency for mismatches between LTR alignments (see Methods). We found intraelement GCEs in 55% of *P. abies* LTR-RTs from fosmids (Figure 3). In the 1.0 genome assembly, we observed GCEs in 36% of LTR-RTs, affecting 40% of Ty3-*gypsy* elements and 27% of Ty1-*copia* elements. The lower percentage of GCEs in the *P. abies* genome assembly is downward biased; the fraction of repetitive sequence within fosmid assemblies is more closely approximating that inferred to be in the *P. abies* genome *in vivo* than does the lower fraction of repetitive sequence observed in the genome assembly (Nystedt, et al. 2013).

In angiosperms a lower fraction of LTR-RTs showed signs of gene conversion compared to *P. abies* fosmids, again with the exception of *Z. mays*, with an average of 23% of LTR-RTs across all studied angiosperms. This ranged from a single GCE observed in *A. thaliana* up to 40% elements with GCEs in *Z. mays* (Figure 3). Parallel differences in levels of gene conversion were also observed when comparing GENECONV analyses with varying stringency levels. Perfectly identical and presumably more recent gene conversion segments (*Gscale* = 0), were observed in 34% of *P. abies* fosmid LTR-RTs (Figure 3) and 16% of assembly LTR-RTs, while in angiosperms, conversion segments were identified in 5-30% of LTR-RTs, with *A. thaliana* and *Z. mays* again at the extremes of this frequency spectrum (Figure 3) and only *Z. mays* approaching the frequency observed in *P. abies*. GENECONV analyses with the lowest stringency threshold (*Gscale* = 1) resulted in slight increases of the proportion of converted elements, with the notable exception of the *P. abies* LTR-RTs from the genome assembly (Figure 3).

Despite the high fraction of observed GCEs in some species, conversion segments in all species were relatively short, and ranged between 222 and 428 bp except in rice (Figure S1). As expected, higher-stringency GENECONV analyses detected much shorter stretches of perfectly identical conversion segments between LTRs, and revealed especially short segments in the two genomes with the oldest elements, *A. trichopoda* and *P. abies*.

The structure and sequence composition of converted and non-converted LTR-RTs and their LTRs were further inspected to disentangle the possible role of these local features in promoting GCEs. Across most species, longer full-length elements, and especially longer LTRs were associated with gene conversion, with the exception of *B. distachyon* for both traits and *Z. mays* for LTR length (Figure 4A, B). In line with these findings, the alignments used to detect GCEs are much longer in converted versus non-converted LTRs of most species (Figure 4C). Thus there could be bias in the GENECONV analyses toward increasing the number of detected gene conversion events in longer elements, because longer alignments tend to contain more overall substitutions than shorter ones, which in turn increases the statistical power for detection. However, this association is absent in *B. distachyon* and *Z. mays*, which show similar alignment lengths in converted and non-converted LTRs. A comparable trend was observed for the ratio of LTR length to internal length (Figure 4D). Overall, the length of LTR-RTs and LTRs appears to be a major determinant of the frequency of GCEs in *P. abies* and in most examined angiosperms.

The sequence identity was similar in converted LTRs compared to non-converted LTRs, including for LTRs in Norway spruce and *A. trichopoda* which showed notably lower overall identity than in the other studied species (Figure 4E). This is counter to the trend typically observed between gene copies, for which paralogous genes with GCEs tend to share higher sequence similarity than non-converted paralogs (Xu, et al. 2008; Casola, et al. 2010). Taken together with the length-related results above, this suggests the gene conversion events we observed within LTR-RTs may have been facilitated primarily by LTR length, rather than sequence similarity. As for the M/U ratio, we did not find a significant difference in GC-content between converted and non-converted LTRs (Figure 4F).

One possible source of bias resulting from an interaction of GCEs and mapping success could be due to gene conversion events between internal regions of LTR-RTs and the flanking DNA of these elements (Vitte and Panaud 2003; Ma, et al. 2005). If common, such events could skew the proportion of mapped reads onto full-length LTR-RT sequences compared to solo LTR-RTs. However, only 3/77 full-length elements were found to show evidence of internal-to-flanking DNA gene conversion in one study (Vitte and Panaud 2003), whereas a single example was described among 53 LTR-RTs analyzed in the orthologous *Orp* regions of maize, sorghum and rice (Ma, et al. 2005). The low frequency of gene conversion between internal LTR-RT sequences and their flanking regions observed in these studies suggests that this process is unlikely to have introduced a significant bias in our mapping data.

This comparison of the structure and composition of converted and non-converted LTR-RTs and their LTRs indicates that while these factors may be important in determining when individual GCE events may occur, as has also been found by other studies already cited, these factors do not differ systematically among our studied species in a manner that could explain the differences we observe in GCE events in large plant genomes (Figure 3).

Largest genomes have lowest fractions of solo-LTRs and highest rates of GCEs

Considering the solo-LTR to complete LTR-RT fractions and LTR-RT-associated GCE rates together (Figure 5), these rates are positively correlated in the species with small- to medium-sized genomes (*Arabidopsis thaliana* to *Amborella trichopoda*; $n = 6$, Spearman's $r_s = 0.841$, $p = 0.036$) while the correlation reverses and weakens to nonsignificance when including the large-genome species *Zea mays* and *Picea abies* ($n = 8$, Spearman's $r_s = -0.216$, $p = 0.61$). As unequal recombination and gene conversion are both homology-driven processes which differ in whether they do or do not resolve in crossing-over, this suggests the possibility that resolution via crossing-over around LTR-RTs occurs at much lower rates in large-genomed species.

Discussion

Our results indicate that general, genome-wide differences in the resolution of LTR-RT-associated recombinative events covary with plant genome size. For gene conversion events, this is a positive and roughly linear relationship, with the highest rates in the largest genomes (Figure 3). For unequal recombination leading to solo-LTRs, our results suggest the occurrence of two distinct regimes: for small- to medium-sized genomes, rates of solo-LTR production are positively correlated and roughly linear, while rates are much lower in species with larger genomes, on the order of maize or larger (Figure 2). The occurrence of two distinct regimes is even more apparent when the rates are plotted together, for those species in which both were estimated (Figure 4).

The degree of solo-LTR under-representation in conifers shows some variability between different LTR-RT groups, but this variation does not significantly correlate with any of the most evident structural features of LTR-RTs in *P. abies*. This contrasts with previous results in angiosperms showing positive correlations between LTR-associated UR and LTR length-related features (Vitte and Panaud, 2003; Du, et al. 2012; El Baidouri and Panaud, 2013), as well as our observed frequency of GCEs, which positively correlates with lengths of element features (Figure 4A). The highest levels of LTR-RT-associated GCEs were observed in the genomes of the two species where LTR-associated UR appears to be most strongly suppressed, which were also the two studies species with the largest genomes: *P. abies* and maize (Figure 5).

The contextual suppression of UR may be achieved via several potentially co-occurring processes, including reduction in homologous recombination via reduced numbers of double-stranded breaks, a preference for non-homologous DNA repair pathways such as IR, and the favoring of alternative outcomes of homologous recombination that do not result in crossing-over, in particular gene conversion. Our results support the existence of this latter process in plants with large genomes. One mechanism that could underly this process would be the formation of heterochromatin in LTR-RT-rich regions via methylation. Evidence supporting a possible role of methylation in limiting and/or controlling the recombination processes has been collected in both animals and plants, albeit limited to particular cellular developmental stages such as meiosis. DNA methylation can restrain TEs from adopting chromatin features amenable to meiotic recombination in mice (Zamudio, et al. 2015). In the germ line of honeybees, methylated genes show a reduced rate of crossing-over (CO) events (Wallberg, et al. 2015). Similarly, DNA methylation and chromatin states were identified as key factors in explaining the striking variation of meiotic CO rate along *Arabidopsis thaliana* chromosomes (Colomè-Tatchè, et al. 2012; Mirouze, et al. 2012). Yelina et al. (2015) demonstrated that DNA methylation has a pivotal role in establishing domains of meiotic recombination along chromosomes and it is sufficient to silence CO hot spots in *Arabidopsis*.

Genome size-associated differences in the regulation of LTR-RT-associated heterochromatin which thereby affects recombination seems the most plausible mechanism which could explain our results. Alternatively, there may exist significant differences in the regulation of the recombination process between seed plants with small- to medium-sized genomes and those with large, LTR-RT-rich genomes. In favor of a heterochromatin-based mechanism, we would predict that genome-wide methylation levels would covary with rates of LTR-RT-associated GCEs, not only in plants with large genomes but also in other taxa. Methylation is certainly elevated in the genomes of conifers, occurring at more than 83% of the total cytosines in *Picea abies* (Ausin et al., 2016) and at more than 64.4% of the cytosines analyzed in *Pinus pinea* (Saez-Laguna, et al. 2014) and is consistently higher than that of other annual and perennial plants (Avramidou, et al. 2015, Ausin et al, 2016).

Other factors may contribute to the observed variation in GCEs between species. For instance, the retroelements sampled from species with higher rates of GCEs may experience particularly high frequency of gene conversion compared to other LTR-RT families. Given that we selected several distantly related families from each species for our analyses, including elements from both Ty3-*gypsy* and Ty1-*copia* groups (Figures S2, S3), this is unlikely to have influenced our results significantly.

A recent study examining a limited number of LTR-RT families in four species of salamanders (Frahry, et al. 2015) has provided similar evidence of a relationship between UR suppression and large genome size. Salamander genomes are huge, having sizes ranging from ~14 Gbp up to ~120 Gbp, this largest over 6 times that of Norway spruce. Low amounts of solo LTRs were detected and no single LTR-RT structural feature was identified as being a strong predictor of solo-LTR underrepresentation (Frahry, et al. 2015). That eukaryotes as evolutionarily far apart as conifers and salamanders share these features regarding LTR-RT removal, with both also characterized by very large genome sizes, is suggestive of a more general mechanism related to the control of TE amplification and removal in large genomes. We predict that these salamander genomes also show an elevated rate of LTR-RT-associated gene conversion events.

Taken together, our results are also consistent with the hypothesis recently put forward by Nina Fedoroff (Fedoroff, 2012) to explain the accumulation of large amounts of repetitive elements in eukaryote genomes despite the presence of mechanisms leading to their removal by unequal or illegitimate recombination. She suggested that TEs can accumulate in huge quantities because of, not in spite of, the epigenetic mechanisms used to control their proliferation. These epigenetic mechanisms maintain heterochromatin where repeats are rich, suppressing the expression and transposition of TEs, but also simultaneously reducing recombinational events that could lead to TE removal. The largest genomes we studied – the four conifers plus maize – are also the genomes with the strongest evidence for suppression of sequence-removing unequal recombination. As the studies cited above indicate in maize and *Drosophila*, heterochromatin does not suppress all forms of recombination, rather just those that lead to crossing-over and hence unequal and illegitimate recombination. While the epigenetic status and the chromatin state within and among the LTR-RT groups were not examined in the present study, our results do suggest an important interplay between LTR-RT content, recombination outcomes and heterochromatin, and are entirely consistent with Fedoroff's hypothesis.

Our results across seed plants emphasize the importance of another prediction arising from Fedoroff's (Fedoroff, 2012) hypothesis. When TE proliferation is more rapid than TE removal, runaway increases in genome size can occur if controls on TE activity develop after proliferation but before significant removal, with the relative balance determined by characteristics of the mechanisms employed to control TE activity. Further investigations of the relationship between epigenetic status, chromatin configuration, and the resolution of homology-dependent recombination in LTR-RT elements across many more taxonomic groups will be required to address the overall impact of transposable elements in genome size evolution across eukaryotes.

Methods

Species sampled

We selected four conifer species and seven angiosperms species for study. The conifers (*Picea abies*, *P. glauca*, *Pinus taeda* and *P. lambertiana*) were the only gymnosperms with sufficient high-quality genomic sequence available at the start of the study. The angiosperms include both monocots and dicots and feature a range of genome sizes. *Arabidopsis thaliana*, *Brachypodium distachyon*, *Oryza sativa*, *Vitis vinifera* and *Zea mays* have each been subject to earlier LTR-RT-related study relevant to facilitating comparisons and evaluating the pipeline described herein. *Amborella trichopoda* is the basal extant angiosperm, while *Populus trichocarpa* has a high-quality genome and complete LTR-RT elements had been previously identified (Natali, et al. 2015). Though the conifers examined include two congeneric pairs, the species are separated by considerable divergence time estimates that vary from the early Miocene for *Picea abies* and *P. glauca* (~14-20 Mya, Nystedt, et al. 2013), around the origin of the genus *Oryza* (Zou, et al. 2013), to the early Cretaceous for *Pinus taeda* and *P. lambertiana* (~110-140 Mya, Saladin, et al. 2017), roughly at the separation of the *Amborella* lineage from all other angiosperms (Amborella Genome Project. 2013).

Identifying LTR-RT groups in *P. abies*

LTR-RT groups were identified on the basis of phylogenetic analyses. Reverse Transcriptase (RT) domains 100 amino acids long (Table S4) were used as queries in tBlastN searches of 100,000 *P. abies* 454 random sheared reads (ftp://congenie.org/Data/ConGenIE/) (Sundell, et al. 2015). All significant hits (E-value < 1e-5) longer than 80 residues were retrieved, totalling 670 and 1410 paralogous sequences for each of the Ty1-*copia* and Ty3-*gypsy* superfamilies, respectively. Sequences were aligned separately for each superfamily using the software MUSCLE (Edgar, 2004). The alignments (Supporting Datasets S2 and S3) were then used to build Neighbor-Joining phylogenetic trees using the software MEGA6 (Tamura, et al. 2013). Overall we identified 7 Ty1-*copia* and 16 Ty3-*gypsy* groups supported by high bootstrap values (Figure S2). We calculated the evolutionary divergence between identified LTR-RT groups using the Poisson-corrected number of amino acid substitutions per site ($\hat{d}$), averaged over all pairwise comparisons between groups as implemented in MEGA6 (Tamura, et al. 2013). As expected, the evolutionary divergence between groups is greater than that within groups for all groups tested (Table S8). A representative reverse transcriptase sequence for each of the 23 groups was used to search the *Picea abies* assembly scaffolds longer than 50 kbp using tBlastN (Camacho, et al. 2009). Regions surrounding the best positive matches were inspected using dot-plot analyses (Sonnhammer and Durbin, 1995) to identify regions containing complete LTR-RT elements. At least five complete LTR-RT elements for each group were identified and retrieved (Table S5).

Representative sequences for these and all other complete LTR-RT elements identified in studied species are provided in Supporting Dataset S1.

Identifying elements in *Picea glauca*, *Pinus taeda* and *P. lambertiana*

A subset of the 23 LTR-RT groups identified in *P. abies* including four Ty3-*gypsy* and five Ty1-*copia* groups was further investigated in *P. glauca*. Included in this subset were the seven most abundant groups identified in *P. abies* as well as two Ty3-*gypsy* groups that were medium-abundant in *P. abies*. Complete LTR-RTs representing paralogous groups were identified by searching the *P. glauca* genome assembly sequence

(Birol, et al. 2013) using the LTR sequence of *P. abies* LTR-RT elements as query in similarity searches followed by dot plot analysis (Sonnhammer and Durbin, 1995).

We manually searched 111 fully sequenced *P. taeda* BACs (Genbank accession numbers: AC241263-AC241362, GU477256, GU477266, HQ141589) (Kovach, et al. 2010) for the presence of LTR-RTs using dot plot analysis (Sonnhammer and Durbin, 1995). 112 complete LTR-RT elements were identified, LTRs were aligned and the alignments were used to build Neighbor-Joining trees for phylogenetic analysis, similarly to what was done for *Picea abies* above. Note that LTRs were used to build the trees for *Pinus taeda*, while RT sequences were used in *Picea abies*; LTRs were used here because the number of elements considered was small enough to allow for manual curation. Complete elements were arranged into 16 groups on the basis of LTR sequence similarity, and the nine most abundant groups were chosen for further investigation.

LTRs of representative elements of the nine LTR-RT groups selected in *P. taeda* were used to search 964,817 *P. lambertiana* contigs longer than 15 kb (http://dendrome.ucdavis.edu/ftp/Genome_Data/genome/pinerefseq/Pila/v1.0/pila.v1.0.scafSeq.gz). Representative elements for each of the nine groups in *P. lambertiana* were identified by dot plot analysis.

Identifying elements in angiosperm genomes

For *Populus trichocarpa*, full length LTR-RTs were from (Natali, et al. 2015). Full length LTR-RTs were downloaded from Repbase (Jurka, et al. 2005) for *Arabidopsis thaliana*, *Amborella trichopoda*, *Brachypodium distachyon*, *Oryza sativa*, *Vitis vinifera* and *Zea mays*. These LTR-RTs were used to evaluate their abundance in the respective host genome using RepeatMasker (Smit, et al. 2015) to search the corresponding genome assemblies. From three to five complete copies from each of the most abundant LTR-RTs group identified were retrieved for use in further analyses.

Estimating the ratio of solo-LTRs to complete LTR-RT elements

For each of the targeted LTR-RT group identified in the different species analyzed, we used the following strategy to infer the ratio of complete LTR-RTs to solo-LTRs, with the numbering of each step corresponds to that illustrated in Figure 1:

I. We retrieved from 3 to 15 complete LTR-RT paralogs from the host genome for each group as described above.

II. For each complete element from (I) we extracted the first 50 nt of the 5' LTR and the last 50 nt of the 3' LTR. We refer to these LTR-RT-derived sequences as *tags*, in particular START tags for those originating from the 5' of the element and END tags for those originating from the 3' end of the element. If no divergence has occurred between LTRs of an inserted element and thus the LTRs remain identical in sequence, the START and END tags would each match both LTRs perfectly.

III. Tags were mapped onto Illumina reads derived from the host genome using RepeatMasker (Smit, et al. 2015).

IV. Reads from (III) were filtered, retaining all the matches which met the following conditions: for START tags, the longest unmatched regions were 3 and 5 nucleotides at the 5' and 3' ends, respectively; for END tags, the longest unmatched regions were 5 and 3 nucleotides at the 5' and 3' ends, respectively. For each matching read passing filtering, we extracted a 20 nt region we call a *tract*. For START tags the START tract included 5 nt from the 5' end of the LTR together with the upstream 15 nt; for END tags the END tract included 5 nt from the 3' end of the LTR together with the downstream 15 nt. Constructed in this way, a START tract will include interior sequence from a complete LTR-RT when the START tag from which it is derived matches the 3' LTR of the complete LTR-RT, while for an END tract, this is true when it matches the 5' LTR of a complete LTR-RT.

V. Tracts were then mapped using BWA ALN (Li and Durbin, 2009) onto the complete LTR-RT paralog sequences used in (I), with the settings k=2, n=4, l=12.

VI. The numbers of mapped (M) and unmapped (U) tracts were determined from BWA output and used to infer relative genomic content of complete LTR-RT elements and solo-LTRs.

Genomic reads covering a complete LTR-RT should, on average, produce the same amount of mapped and unmapped tracts, whereas genomic reads covering a solo-LTR should produce only unmapped tracts. The amount of mapped versus unmapped tags in a genome mostly containing complete LTR-RTs should be approximately equal, resulting in an M/U ratio of approximately 1. On the other hand, the presence of solo-LTRs in the genome should produce a notable reduction of this ratio from 1. There may be a bias toward unmapped reads, depending on the degree of divergence among genomic LTR-RTs; this can be controlled by ensuring START and END tags are derived from a variety of LTR-RT paralogs. We have endeavoured to be comprehensive for the groups studied, nevertheless a general caution for all genomic analyses of repetitive elements also applies here: because related elements within the same genome can show quite remarkable divergence, the results should be considered to be characteristic of the specific LTR-RT groups studied. Note also that some LTR-RT paralogs retrieved from assemblies contained N-gaps (Supporting Dataset S1); in all cases these gaps are not present at LTR borders, thus they do not affect this analysis.

The ratios of solo-LTRs (S) per complete LTR-RT (C), as well as the reciprocal ratio of complete LTR-RTs per solo-LTR, can be quantified using the relations:

$$\frac{S}{C} = \frac{U}{M} - 1, \frac{C}{S} = \frac{M}{U - M}$$

The pipeline was run for each species analyzed, using a whole-genome shotgun Illumina reads dataset assumed to represent an unbiased sample of each genome (see Table S1 for ENA accession numbers). For most read sets, a subset of reads were used; additionally, for paired-end datasets, only the first read of each pair was used. The amounts of read sequence used from each read set and relative genomic coverage provided by each reads dataset are also detailed in Table S1.

Pipeline validation

The reliability of the above pipeline was tested in *Picea abies* and *Pinus taeda* using alternative approaches and other data sources. In *Picea abies*, we randomly selected 4,348 sequences (175 Mbp in total, provided in Supporting Dataset S4) from a large collection of fosmid pool scaffolds and estimated the M/U ratio for the Ty3-*gypsy* group *Alisei*. Each fosmid pool contained ~40 Mbp of fosmid sequence, representing ~0.2% of the total genome of *P. abies*, and is more representative of the true content of repetitive sequences in the genome than is the whole-genome shotgun assembly (Nystedt, et al. 2013). The assembled fosmid sequences were manually searched for the presence of *Alisei* LTRs using dot plot analyses (Sonnhammer and Durbin, 1995). We identified 171 complete elements and 18 solo-LTRs, giving an M/U ratio (0.90) consistent with the one estimated by the pipeline (0.89).

In *Pinus taeda*, representative LTRs from each LTR-RT group were also used to manually search the previously mentioned 111 fully sequenced BACs (totalling ~11 Mbp) (Kovach, et al. 2010) using dot plot analysis (Sonnhammer and Durbin, 1995). Positive matches were checked to see if they belonged to a complete LTR-RT or to a solo-LTR. In total 243 sites were identified: 187 complete LTR-RTs and 56 solo-LTRs. These figures translated to a M/U ratio of 0.77 that is somewhat less than the pipeline estimate of 0.88.

The underestimation of the M/U ratio for *Pinus taeda*, in contrast to the close agreement for *Picea abies*, could simply be a stochastic effect of a lesser amount of high-quality sequences available for *Pinus taeda* vs. *Picea abies* (11 Mbp vs. 175 Mbp). Our restriction of the search in *P. abies* to a single LTR-RT group (*Alisei*) might have compensated for this to some degree, as indicated by the similar numbers of complete elements recovered, but this also could have allowed for greater tolerance for divergence when recovering solo-LTRs and thus greater relative numbers of solo-LTRs within the *Pinus taeda* BACs (see below), where this restriction was not applied. Nevertheless, for both species validation data provide further support for a strong under-representation of solo-LTRs.

We also specifically tested the accuracy of pipeline step (III) which maps tags onto Illumina reads using RepeatMasker. In particular, we evaluated the average similarity of the positive matches as well as the fraction of positive matches having a similarity value smaller than 80%. The latter fraction could include artefactual matches to very divergent elements or unrelated elements. The overall similarity is above 90% for all species with the exception of *Amborella trichopoda* at 87.84% (Table S6). These values are well above the lowest similarity value (80%) proposed by Wicker et al. (2007) for defining a LTR-RT family. Furthermore the fraction of matches having similarity lower than 80% is quite limited, usually under 2% of the total, with the highest value reaching 2.38%, again in *A. trichopoda* (Table S6).

We evaluated the potential for tracts to be erroneously classified as "unmapped" during pipeline step (V) by collecting all unmapped tracts and clustering them using CD-HIT (Fu et al., 2012). Our reasoning is that unmapped tracts should reflect the random distribution of sequences adjacent to LTR-RT insertions and therefore should mostly differ from each other. Any large cluster of highly similar unmapped sequences would be suggestive of artefactual errors. We screened all of our unmapped tracts for such instances and no suspicious cases were identified (results not shown).

We also evaluated the potential for biases in mapping percentages during pipeline step (V) introduced by the generation of START and END tags from different ends of representative retroelements. If cases of element truncation are common, a clear difference in the mapped/unmapped (M/U) ratios should be apparent when calculated using tracts derived from START and END tags separately. In the overall majority of the cases for both angiosperms and gymnosperms, these ratios are in very good agreement and we observed no systematic bias involving tags from either origin nor in gymnosperms vs. angiosperms (Table S7).

We also considered the possible confounding effect of differences in relative genomic coverage provided by reads datasets among the studied species, as this negatively covaries with genome size (Table S1), an important factor in our conceptual models. We attempted to separate these effects by evaluating linear models in which M/U ratio was dependent upon on both relative coverage and genome size. A fully specified model showed neither coverage, genome size, nor their interaction to be individually significant ($p > 0.24$ for genome size, $p > 0.75$ for coverage and interaction) though the full model was ($F_{3,112} = 17.45$, $p < 1\text{x}10^{-8}$). Dropping the interaction term did not significantly weaken the model (likelihood ratio test, $p = 0.89$), and a model lacking the interaction term showed genome size to be a significant predictor of M/U ($p < 1\text{x}10^{-5}$) while relative coverage was not (p > 0.74). Though sample size is limited, we interpret these results to indicate that genome size is a predictor of M/U and relative coverage is not.

Finally, we compared our estimated solo-LTR to complete LTR-RT ratios with the literature, which included five of the seven angiosperm species considered in this study (Table S9). Our results are in good agreement with those calculated in *Z. mays* by SanMiguel et al. (1996) and El Baidouri and Panaud (2013), with those calculate in *O. sativa* by Ma et al (2004) and El Baidouri and Panaud (2013) and with those assessed in *B. distachyon* by El Baidouri and Panaud (2013). The most apparent discrepancy was seen for *V. vinifera*, for which we report a slight excess of solo-LTRs (ratio 1.28) while El Baidouri and Panaud (2013) report a slight deficit (ratio 0.84). It is however important to consider that data available in literature were obtained using a wide array of different strategies as well as varying definitions of solo-LTRs. Because of this, the direct comparisons of data from such different sources is not straightforward.

During revision, we learned of a similar method employing LTR-RT-derived tags described by Macas, et al. (2015) when examining genome size variation in the legume tribe Fabeae. Though methodological details differ and our sampling of representative LTR-RTs, tag sites, and pipeline validation are more extensive, we would expect that both methods would produce broadly similar results. We would expect our method to be more stable when applied to taxa such as conifers, in which transposable elements can be quite old and diverged, where a Blast-based method might produce an unreasonably large number of element groups; we have not subjected this to test.

Intraelement LTR gene conversion

Gene conversion events (GCEs) between LTRs of complete elements were detected using the software GENECONV (Sawyer, 1999). We identified a total of 137 complete elements from angiosperm genomes and 353 complete elements from the *P. abies* 1.0 genome assembly (Nystedt, et al. 2013) and fosmid pool assemblies (295 elements from the genome assembly and 58 elements from fosmids) using the same method as that described above to identify complete LTR-RT elements in *P. abies*. Each LTR sequence was extracted from the full-length copy element using BEDTools (Quinlan and Hall, 2010) and the two LTRs of each element were compared locally against each other using BLAST+ 2.2.29 (Camacho, et al. 2009) with the following settings: blastn –task blastn –dust no –evalue 1e-05. Alignments from the BLASTN results were parsed using custom Perl scripts and utilized to search for gene conversion segments using GENECONV (Sawyer, 1999). Through permutation analyses of sequence alignments, GENECONV determines the probability that regions of the alignment showing a high level of nucleotide similarity derive from gene conversion events rather than stochastic variation of nucleotide substitutions. Recent gene conversion events appear as stretches of identical nucleotides in alignments of homologous sequences; converted segments derived from older GCEs tend to accumulate substitutions between the donor and acceptor sequences, thus appearing as shorter identical stretches interrupted by single-nucleotide substitutions or larger indels in the alignments.

The following GENECONV settings were used: /w123 /lp /f /eb /g0 [or /g1 or /g2] -include_monosites. These settings allowed to search for gene conversion segments in alignments with two sequences only and to consider run of missing data sites or indel sites as single ‘polymorphisms’. Each aligned sequence was run through GENECONV three times with three different values for the gscale (g) option: 0, 1 and 2. The gscale value determines the mismatch penalties associated with conversion segments. A gscale value of 0 allows no mismatches in the segments, gscale 1 applies the lowest mismatch penalties and often results in more segments being detected, and gscale 2 applies more strict mismatch penalties and tends to identify a number of segments intermediate between the results of gscale 0 and 1 (Sawyer, 1999). Segments discovered using different gscale values usually overlapped, although segments observed with gscale 0 tend to be shorter and to represent younger GCEs, while segments identified using gscale 1 tend to be the longest and could represent older segments that have accumulated more mismatches.

Acknowledgements

This project was funded by Scuola Superiore Sant'Anna, Pisa, Italy (grant reference APOMIS11AZ). The Norway spruce genome project together with *P. abies* fosmids sequencing was originally supported by the Knut and Alice Wallenberg Foundation. Some computations were performed on resources provided by UPPNEX/SNIC through the Uppsala Multidisciplinary Center for Advanced Computational Science (UPPMAX) project b2010042. We are grateful to Alexander Suh for helpful discussions, and to the anonymous referees for helpful comments that greatly improved the paper.

Disclosure Declaration

All authors declare no conflict of interest.

References

Amborella Genome Project. 2013. The *Amborella* genome and the evolution of flowering plants. *Science* **342:** 1241089. doi:10.1126/science.1241089

Ausin I, Feng S, Yu C, Liu W, Kuo HY, Jacobsen EL, Zhai J, Gallego-Bartolome J, Wang L, Egertsdotter, U Street NR, Jacobsen SE, Wang H. 2016. DNA Methylome of the 20-gigabase Norway spruce genome. *Proc Natl Acad Sci USA* published ahead of print November 28, 2016, doi:10.1073/pnas.1618019113

Avramidou EV, Doulis AG, Aravanopoulos FA. 2015. Determination of epigenetic inheritance, genetic inheritance, and estimation of genome DNA methylation in a full-sib family of *Cupressus sempervirens* L. *Gene* **562:** 180-187.

Baucom RS, Estill JC, Chaparro C, Upshaw N, Jogi A, Deragon JM, Westerman RP, SanMiguel PJ, Bennetzen JL. 2009. Exceptional diversity, non-random distribution, and rapid evolution of retroelements in the B73 maize genome. *PLoS Genet* **5:** e1000732.

Bennett MD, Leitch IJ. 2012. Plant DNA C-values Database (Release 6.0, Dec. 2012). Available: http://data.kew.org/cvalues/. Last Accessed 20 April 2016.

Birol I, Raymond A, Jackman SD, Pleasance S, Coope R, Taylor GA, Yuen MM, Keeling CI, Brand D, Vandervalk BP, et al. 2013. Assembling the 20 Gb white spruce (*Picea glauca*) genome from whole-genome shotgun sequencing data. *Bioinformatics* **29:** 1492-1497.

Bucher E, Reinders J, Mirouze M. 2012. Epigenetic control of transposon transcription and mobility in Arabidopsis. *Curr Opin Plant Biol* **15**: 503-510.

Buschiazzo E, Ritland C, Bohlmann J, Ritland K. 2012. Slow but not low: genomic comparisons reveals slower evolutionary rate and higher dN/dS in conifers compared to angiosperms. *BMC Evol Biol* **12:** 8

Camacho C, Coulouris G, Avagyan V, Ma N, Papadopoulos J, Bealer K, Madden TL. 2009. BLAST+: architecture and applications. *BMC Bioinformatics* **10:** 421-429.

Casola C, Ganote CL, Hahn MW. 2010. Nonallelic gene conversion in the genus *Drosophila*. *Genetics* **185:** 95-103.

Casola C, Conant GC, Hahn MW. 2012. Very low rate of gene conversion in the yeast genome. *Mol Biol Evol* **29:** 3817-3826.

Chen J-M, Cooper DN, Chuzhanova N, Ferec C, Patrinos GP. 2007. Gene conversion: mechanisms, evolution and human disease. *Nat Rev Genet* **8:** 762-775.

Chiolo I, Minoda A, Colmenares SU, Pollyzos A, Costes SV, Karpen GH. 2011. Double-strand breaks in heterochromatin move outside of a dynamic HP1a domain to complete recombinational repair. *Cell* **144:** 732-744.

Colomé-Tatché M, Cortijo S, Wardenaar R, Morgado L, Lahouze B, Sarazin A, Etcheverry M, Martin A, Feng S, Duvernois-Berthet E, et al. 2012. Features of the *Arabidopsis* recombination landscape resulting from the combined loss of sequence variation and DNA methylation. *Proc Natl Acad Sci USA* **109:** 16240-5.

Devos KM, Brown JK, Bennetzen JL. 2002. Genome size reduction through illegitimate recombination counteracts genome expansion in *Arabidopsis*. *Genome Res* **12:** 1075–1079.

Dooner HK, Martinez-Ferez IM. 1997. Recombination occurs uniformly within the bronze gene, a meiotic recombination hotspot in the maize genome. *Plant Cell* **9:** 1633-1646.

Drouin G. 2002. Characterization of the gene conversions between the multigene family members of the yeast genome. *J Mol Evol* **55:** 14-23.

Du J, Tian Z, Hans CS, Laten HM, Cannon SB, Jackson SA, Shoemaker RC, Ma J. 2012. Evolutionary conservation, diversity and specificity of LTR-retrotransposons in flowering plants: insights from genome-wide analysis and multi-specific comparison. *Plant J* **63:** 584-598.

Dubcovsky J, Ramakrishna W, SanMiguel PJ, Busso CS, Yan L, Shiloff BA, Bennetzen JL. 2001. Comparative sequence analysis of colinear barley and rice bacterial artificial chromosomes. *Plant Physiol* **125:** 1342-53.

Edgar RC. 2004. MUSCLE: multiple sequence alignment with high accuracy and high throughput. *Nucleic Acids Res* **32:** 1792-1797.

El Baidouri M, Panaud O. 2013. Comparative genomic paleontology across plant kingdom reveals the dynamics of TE-driven genome evolution. *Genome Biol Evol* **5:** 954-965.

Fedoroff NV. (2012) Presidential address. Transposable elements, epigenetics, and genome evolution. *Science* **338**:758-67.

Feschotte C, Jiang N, Wessler SR. 2002. Plant transposable elements: where genetics meets genomics. *Nat Rev Genet* **3:** 329–341.

Frahry MB, Sun C, Chong RA, Mueller RL. 2015. Low levels of LTR retrotransposon deletion by ectopic recombination in the gigantic genomes of salamanders. *J Mol Evol* **80:** 120-129.

Fu H, Dooner HK. 2002. Intraspecific violation of genetic colinearity and its implications in maize. *Proc Natl Acad Sci USA* **99:** 9573-8.

Fu L, Niu B, Zhu Z, Wu S, Li W. 2012. CD-HIT: accelerated for clustering the next generation sequencing data. *Bioinformatics* **28:** 3150-3152.

Guo H, Wang X, Gundlach H, Mayer KF, Peterson DG, Scheffler BE, Chee PW, Paterson AH. 2014. Extensive and biased intergenomic nonreciprocal DNA exchanges shaped a nascent polyploid genome, *Gossypium* (cotton). *Genetics* **197:** 1153-1163.

Hawkins HS, Proulx SR, Rapp RA, Wendel JF. 2009. Rapid DNA loss as a counterbalance to genome expansion through retrotransposon proliferation in plants. *Proc Natl Acad Sci USA* **106:** 17811-6.

International Brachypodium Initiative. 2010. Genome sequencing and analysis of the model grass *Brachypodium distachyon*. *Nature* **463:** 763-768.

International Rice Genome Sequencing Project. 2005. The map-based sequence of the rice genome. *Nature* **436:** 793-800.

Jaillon O, Aury JM, Noel B, Policriti A, Clepet C, Casagrande A, Choisne N, Aubourg S, Vitulo N, Jubin C, et al. 2007. The grapevine genome sequence suggests ancestral hexaploidization in major angiosperm phyla. *Nature* **449:** 463-467.

Jurka J, Kapitonov VV, Pavlicek A, Klonowski P, Kohany O, Walichiewicz J. 2005. Repbase Update, a database of eukaryotic repetitive elements. *Cytogenet Genome Res* **110:** 462-467.

Kejnovsky E, Hobza R, Kubat Z, Widmer A, Marais GA, Vyskot B. 2007. High intrachromosomal similarity of retrotransposon long terminal repeats: evidence for homogenization by gene conversion on plant sex chromosomes? *Gene* **390:** 92-97.

Li H, Durbin R. 2009. Fast and accurate short read alignment with Burrows-Wheeler Transform. *Bioinformatics* **25:** 1754-60.

Li L, Jean M, Belzile F. 2006. The impact of sequence divergence and DNA mismatch repair on homeologous recombination in *Arabidopsis*. *Plant J* **45:** 908-916.

Lippman Z, Gendrel A-V, Black M, Vaughn MW, Dedhia N, Richard McCombie W, Lavine K, Mittal V, May B, Kasschau KD, et al. 2004. Role of transposable elements in heterochromatin and epigenetic control. *Nature* **430**: 471-476.

Lu Y, Ran J-H, Guo D-M, Yang Z-Y, Wang X-Q. 2014. Phylogeny and divergence times of gymnosperms inferred from single-copy nuclear genes. *PLoS ONE* **9:** e107679.

Ma J, Devos KM, Bennetzen JL. 2004. Analyses of LTR-Retrotransposon structures reveal recent and rapid genomic DNA loss in rice. *Genome Res* **14:** 860–869.

Ma J, SanMiguel P, Lai J, Messing J, Bennetzen JL. 2005. DNA rearrangement in orthologous orp regions of the maize, rice and sorghum genomes. *Genetics* **170:** 1209-1220.

Macas J, Novák P, Pellicer J, Čížková J, Koblížková A, Neumann P, Fuková I, Doležel J, Kelly LJ, Leitch IJ. 2015. In-depth characterization of repetitive DNA in 23 plant genomes reveals sources of genome size varation in the legume tribe Fabeae. *PLoS ONE* **10:** e0143424.

Miller DE, Smith CB, Kazemi NY, Cockrell AJ, Arvanitakas AV, Blumenstiel JP, Jaspersen SL, Hawley RS. 2016. Whole-genome analysis of individual meiotic events in *Drosophila melanogaster* reveals that noncrossover gene conversions are insensitive to interference and the centromere effect. *Genetics* **203:** 159-171.

Mirouze M, Lieberman-Lazarovich M, Aversano R, Bucher E, Nicolet J, Reinders J, Paszkowski J. 2012. Loss of DNA methylation affects the recombination landscape in *Arabidopsis*. *Proc Natl Acad Sci USA* **109:** 5880-5885.

Mondragon-Palomino M, Gaut BS. 2005. Gene conversion and the evolution of three leucine-rich repeat gene families in *Arabidopsis thaliana*. *Mol Biol Evol* **22:** 2444-2456.

Natali L, Cossu RM, Mascagni F, Giordani T, Cavallini A. 2015. A survey of *Gypsy* and *Copia* LTR-retrotransposon superfamilies and lineages and their distinct dynamics in the *Populus trichocarpa* (L.) genome. *Tree Genet Genomes* **11:** 107.

Neale DB, Wegrzyn JL, Stevens KA, Zimin AV, Puiu D, Crepeau MW, Cardeno C, Koriabine M, Holtz-Morris AE, Liechty JD, et al. 2014 Decoding the massive genome of loblolly pine using haploid DNA and novel assembly strategies. *Genome Biol* **15:** R59.

Nystedt B, Street NR, Wetterbom A, Zuccolo A, Lin Y-C, Scofield DG, Vezzi V, Delhomme N, Giacomello S, Alexeyenko A, et al. 2013. The Norway spruce genome sequence and conifer genome evolution. *Nature* **497:** 579–584.

Paul R, Stevens KA, Martinez-Garcia PJ, Zimin A, Holtz-Morris A, Yorke JA, Koriabine M, Crepeau M, Puiu D, Salzberg SL, et al. 2015. Repeat sequence characterization in sugar pine (*Pinus lambertiana*) and loblolly pine (*Pinus taeda*). Available: http://pinegenome.org/pinerefseq/files/PAG2015_Paul_PineRefSeq.pdf, accessed 10 September 2016.

Pereira, V. 2004. Insertion bias and purifying selection of retrotransposons in the *Arabidopsis thaliana* genome. *Genome Biol* **10:** R79.

Peterson CL. 2011. The ins and outs of heterochromatic DNA repair *Dev Cell* **20:** 285-287.

Quinlan AR, Hall IM. 2010. BEDTools: a flexible suite of utilities for comparing genomic features. *Bioinformatics* **26:** 841-842.

Sáez-Laguna E, Guevara M-Á, Díaz L-M, Sánchez-Gómez D, Collada C, Aranda I, María-Teresa Cervera M-T. 2014. Epigenetic variability in the genetically uniform forest tree species *Pinus pinea* L. *PloS ONE* **9:** e103145. doi:10.1371/journal.pone.0103145

Saladin B, Leslie AB, Wüest RO, Litsios G, Conti E, Salamin N, Zimmermann NE. 2017. Fossils matter: improves estimates of divergence times in *Pinus* reveal older diversification. *BMC Evol Biol* **17:** 95.

SanMiguel P, Tikhonov A, Jin YK, Motchoulskaia N, Zakharov D, Melake-Berhan A, Springer PS, Edwards KJ, Lee M, Avramova Z, Bennetzen JL. 1996. Nested retrotransposons in the intergenic regions of the maize genome. *Science* **274**: 765–768.

SanMiguel P, Gaut BS, Tikhonov A, Nakajima Y, Bennetzen, JL. 1998. The paleontology of intergene retrotransposons of maize. *Nat Genet* **20:** 43 45.

Sawyer SA. 1999. GENECONV: a computer package for the statistical detection of gene conversion. http://www.math.wustl.edu/~sawyer/geneconv/, accessed 10 September 2016.

Schnable PS, Ware D, Fulton RS, Stein JC, Wei F, Pasternak S, Liang C, Zhang J, Fulton L, Graves TA, et al. 2009. The B73 maize genome: complexity, diversity, and dynamics. *Science* **326:** 1112-1115

Sharma A, Wolfgruber TK, Presting GG. 2013. Tandem repeats derived from centromeric retrotransposons. *BMC Genomics* **14:** 142.

Shi J, Wolf SE, Burke JM, Presting GG, Ross-Ibarra J, Dawe RK. 2010. Widespread gene conversion in centromere cores. *PLoS Biol* **8:** e1000327.

Sonnhammer EL, Durbin R 1995. A dot-matrix program with dynamic threshold control suited for genomic DNA and protein sequence analysis. *Gene* **167:** 1-10

Smit AFA, Hubley R, Green P. 2015. RepeatMasker Open-4.0. http://www.repeatmasker.org, accessed 10 September 2016.

Stevens KA, Wegrzyn JL, Zimin A, Puiu D, Crepeau M, Cardeno C, Paul R, Gonzalez-Ibeas D, Koriabine M, Holtz-Morris AE, Martínez-García PJ, Sezen UU, Marçais G, Jermstad K, McGuire PE, Loopstra CA, Davis JM, Eckert A, de Jong P, Yorke JA, Salzberg SL, Neale DB, Langley CH. 2016. Sequence of the Sugar Pine megagenome. *Genetics* **204:** 1613-1626.

Sundell D. Mannapperuma C, Netotea S, Delhomme N, Lin Y-C, Sjödin A, Van de Peer Y, Jansson S, Hvidsten TR, Street NR. 2015. The Plant Genome Integrative Explorer Resource: PlantGenIE.org. *New Phytol* **208:** 1149–1156. doi:10.1111/nph.13557

Talbert PB, Henikoff S. 2010. Centromeres convert but don't cross. *PLoS Biol* **8:** e1000326.

Tamura K, Stecher G, Peterson P, Filipski A, Kumar S. 2013. MEGA6: Molecular Evolutionary Genetics Analysis Version 6.0. *Mol Biol Evol* **30:** 2725-2729. doi:10.1093/molbev/mst197

Trombetta B, Fantini G, D'Atanasio E, Sellitto D, Cruciani F. 2016. Evidence of extensive non-allelic gene conversion among LTR elements in the human genome. *Sci Rep* **6:** 28710. doi:10.1038/srep28710

Tuskan GA, Difazio S, Jansson S, Bohlmann J, Grigoriev I, Hellsten U, Putnam N, Ralph S, Rombauts S, Salamov A, et al. 2006. The genome of black cottonwood, *Populus trichocarpa* (Torr. & Gray). *Science* **313:** 1596-1604

Vicient CM, Suoniemi A, Anamthawat-Jónsson K, Tanskanen J, Beharav A, Nevo E, Schulman AH. 1999. Retrotransposon BARE-1 and its role in genome evolution in the genus *Hordeum*. *Plant Cell* **11:** 1769–1784.

Vitte C, Panaud O. 2003. Formation of solo-LTRs through unequal homologous recombination counterbalances amplifications of LTR retrotransposons in rice *Oryza sativa* L. *Mol Biol Evol* **20:** 528-40.

Vitte C, Panaud O, Quesneville H. 2007. LTR retrotransposons in rice (*Oryza sativa*, L.): recent burst amplifications followed by rapid DNA loss. *BMC Genomics* **6:** 218.

Wallberg A, Glémin S, Webster MT. 2015. Extreme recombination frequencies shape genome variation and evolution in the honeybee, *Apis mellifera*. *PLoS Genet* **11:** e1005189.

Wang H, Liu J-S. 2008. LTR retrotransposon landscape in *Medicago truncatula*: more rapid removal than in rice. *BMC Genomics* **9:** 382.

Wang XY, Paterson AH. 2011. Gene conversion in angiosperm genomes with an emphasis on genes duplicated by polyploidization. *Genes (Basel)* **2:** 1-20.

Wang X, Tang H, Bowers JE, Paterson AH. 2009. Comparative inference of illegitimate recombination between rice and sorghum duplicated genes produced by polyploidization. *Genome Res* **19:** 1026-1032.

Wegrzyn JL, Liechty JD, Stevens KA, Wu LS, Loopstra CA, Vasquez-Gross HA, Dougherty WM, Lin BY, Zieve JJ, Martínez-García PJ, et al. 2014. Unique features of the loblolly pine (*Pinus taeda* L.) megagenome revealed through sequence annotation. *Genetics* **196:** 891-909.

Wicker T, Sabot F, Hua-Van A, Bennetzen JL, Capy P, Chalhoub B, Flavell A, Leroy P, Morgante M, Panaud O, et al. 2007. A unified classification system for eukaryotic transposable elements. *Nat Rev Genet* **8:** 973–982.

Xu S, Clark T, Zheng H, Vang S, Li R, Wong GK, Wang J, Zheng X. 2008. Gene conversion in the rice genome. *BMC Genomics* **9:** 93.

Yelina NE, Lambing C, Hardcastle TJ, Zhao X, Santos B, Henderson IR 2015. DNA methylation epigenetically silences crossover hot spots and controls chromosomal domains of meiotic recombination in *Arabidopsis*. *Gene Dev* **29**: 2183-2202.

Zamudio N, Barau J, Teissandier A, Walter M, Borsos M, Servant N, Bourc'his D. 2015. DNA methylation restrains transposons from adopting a chromatin signature permissive for meiotic recombination. *Gene Dev* **29:** 1256-70.

Zou X-H, Yang Z, Doyle JJ, Ge S. 2013. Multilocus estimation of divergence times and ancestral effective population sizes of *Oryza* species and implications for the rapid diversification of the genus. *New Phytol* **198:** 1155-1164.

Zuccolo A, Scofield DG, De Paoli E, Morgante M. 2015. The Ty1-*copia* LTR retroelement family PARTC is highly conserved in conifers over 200 MY of evolution. *Gene* **568**: 89-99.

Figure Legends

Figure 1. Method to estimate ratio of solo-LTRs to complete LTR-RTs within a species. (I) Retrieve or assemble 3 to 10 paralogs for each LTR-RT group. (II) Extract 50-nt START and END tags from LTRs of paralogs. (III) Find genomic reads matching START and END tags with RepeatMasker (Smit, et al. 2015), allowing for mismatches. (IV) For each matching read, extract a 20-nt tract containing 5 nt from the tag and 15 nt flanking sequence. Tracts are taken from the 5' or 3' ends of START or END tag matches, respectively. (V) Map each tract to the LTR-RT paralogs collected in (I) using BWA ALN (Li and Durbin, 2009), allowing for mismatches. Count the numbers of mapped (M) and unmapped (U) tracts. Genomic reads covering complete LTR-RTs yield tracts that are mapped and unmapped in equal numbers, while genomic reads covering solo LTRs produce only unmapped tracts. (VI) The relative genomic content of solo LTRs to complete LTR-RTs is inferred from the ratio of mapped to unmapped tracts. See Methods for further details and pipeline validation results.

Figure 2. Ratios of solo-LTRs to complete LTR-RT elements, as a proxy for rates of unequal recombination, from seven angiosperm species and four conifer species versus genome size ($\log_{10}$ axis). For each species, ratios for separate LTR-RT groups are shown together with the total ratio of solo-LTRs to complete LTR-RT elements for all tracts. Shown above *B. distachyon*, *V. vinifera* and *O. sativa* are the numbers of LTR-RT groups from each species with ratios that exceed the upper limit of the y-axis. See Table S1 for genome size references and Tables S2 and S3 for all LTR-RT group ratios.

Figure 3. Proportion of examined LTR-RTs with intraelement gene conversion events (GCEs) between LTRs versus genome size ($\log_{10}$ axis). Pooled results for all identified GCEs are shown, together with separate results for *Gscale* parameters in order of increasing stringency against mismatches for detection of GCEs between aligned sequences; see Methods for further details. Species are colored as in Figure 2.

Figure 4. Characteristics of examined LTR-RTs inferred to contain (values on x-axis) or lack (values on y-axis) gene conversion events (GCEs); the diagonal dashed lines represent equal values in both cases. Plotted values are within-species means ± standard error. Separate *P. abies* values are shown for LTR-RTs in fosmid pool assemblies (filled circles) and the genome assembly (open circles); the latter contains a biased, lower proportion of repetitive sequences than the *P. abies* genome *in vivo*, see main text. *Arabidopsis thaliana* is excluded due to just one observed GCE. Species are colored as in Figure 2

Figure 5. Proportion of examined LTR-RTs with intraelement gene conversion events (GCEs) between LTRs versus the total ratio of solo-LTRs to complete LTR-RT elements, as a proxy for rates of unequal recombination. Proportion of GCEs shown is for all identified GCEs (equivalent to solid dots in Figure 3). Species are colored as in Figure 2 and symbol area is proportional to genome size of each species. The correlation among the six small- to medium-genome species is positive (Spearman's $\rho = 0.841$, $r_s = 0.036$) while including the two large-genome species reverses and weakens the correlation to nonsignificance (Spearman's $r_s = -0.216$, $p = 0.61$).

Figure 1

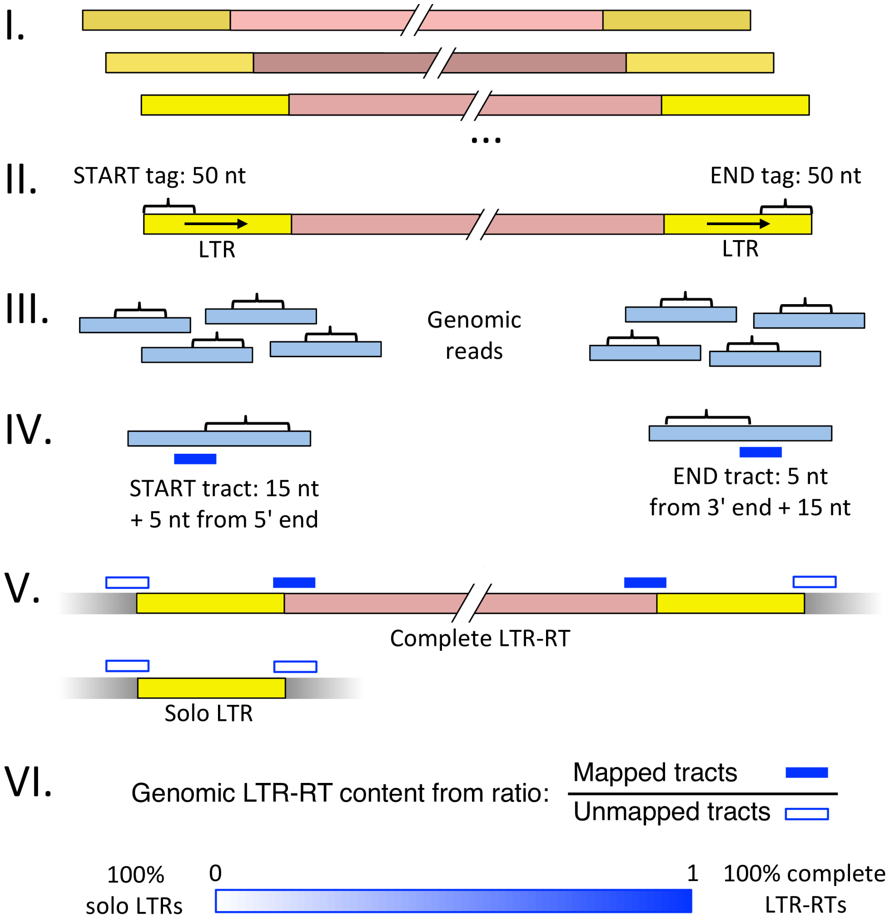
I.
...
II.
START tag: 50 nt
END tag: 50 nt
LTR
LTR
III.
Genomic reads
IV.
START tract: 15 nt + 5 nt from 5' end
END tract: 5 nt from 3' end + 15 nt
V.
Complete LTR-RT
Solo LTR
VI.
Genomic LTR-RT content from ratio:
Mapped tracts
Unmapped tracts
100% solo LTRs
0
1
100% complete LTR-RTs

Figure 2

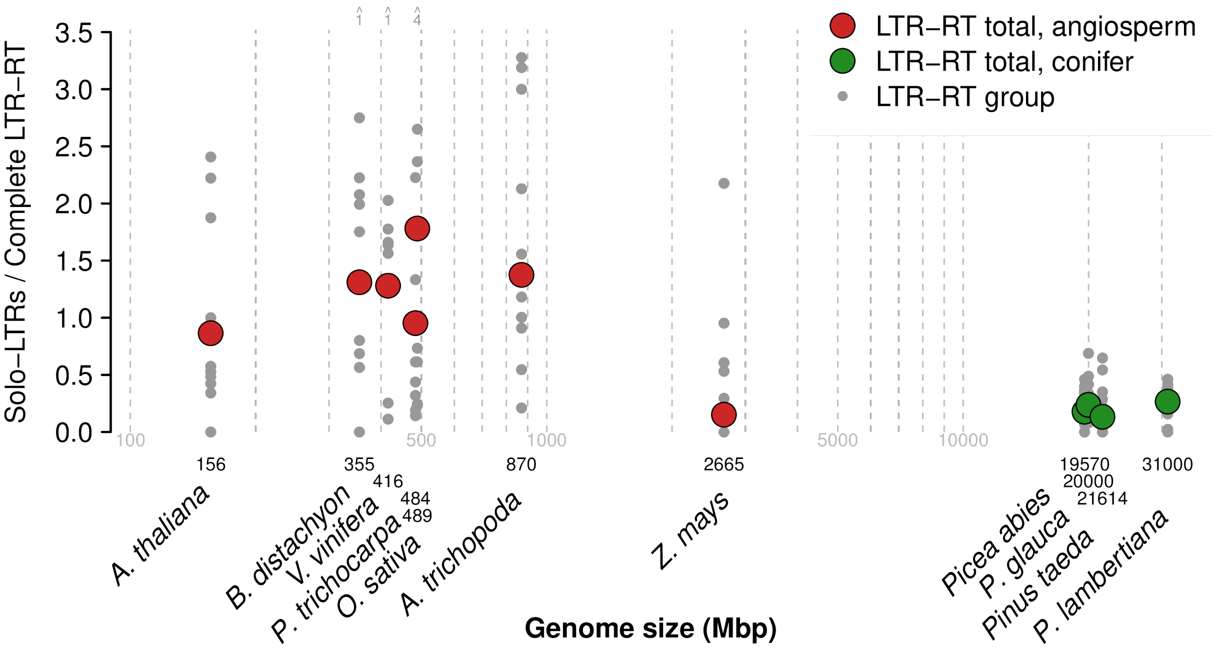
Solo−LTRs / Complete LTR−RT
0.0
0.5
1.0
1.5
2.0
2.5
3.0
3.5
^ 1
^ 1
^ 4
100
500
1000
5000
10000
156
355
416
484
489
870
2665
19570
20000
21614
31000
A. thaliana
B. distachyon
V. vinifera
P. trichocarpa
O. sativa
A. trichopoda
Z. mays
Picea abies
P. glauca
Pinus taeda
P. lambertiana
Genome size (Mbp)
● LTR−RT total, angiosperm
● LTR−RT total, conifer
● LTR−RT group

Figure 3

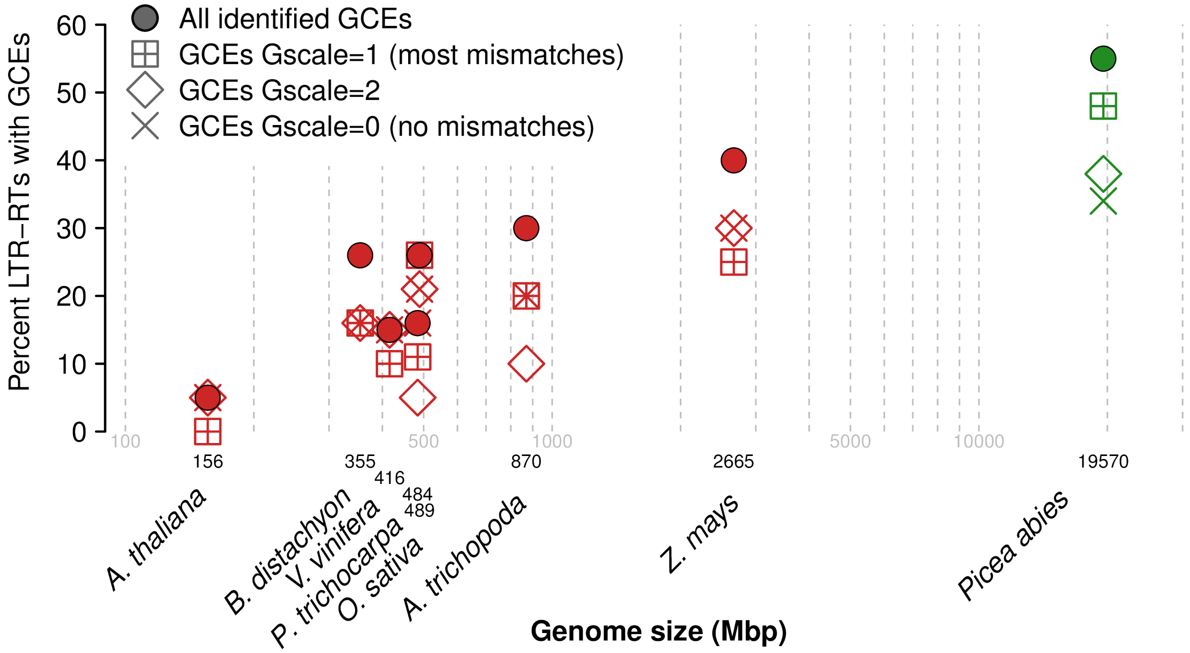
All identified GCEs
GCEs Gscale=1 (most mismatches)
GCEs Gscale=2
GCEs Gscale=0 (no mismatches)
Percent LTR–RTs with GCEs
0
10
20
30
40
50
60
100
500
1000
5000
10000
156
355
416
484
489
870
2665
19570
A. thaliana
B. distachyon
V. vinifera
P. trichocarpa
O. sativa
A. trichopoda
Z. mays
Picea abies
Genome size (Mbp)

Figure 4

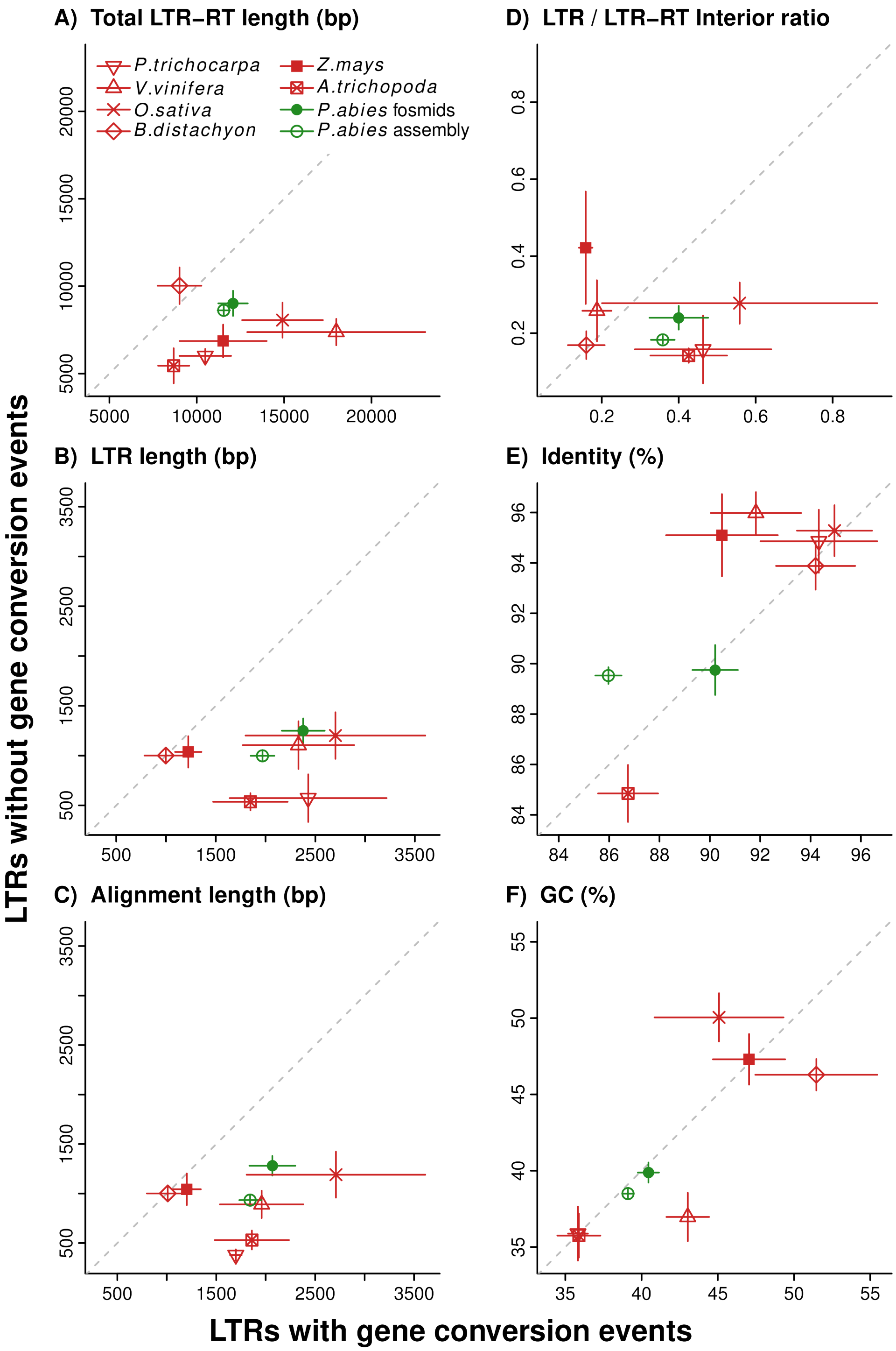
A) Total LTR−RT length (bp)
P.trichocarpa
V.vinifera
O.sativa
B.distachyon
Z.mays
A.trichopoda
P.abies fosmids
P.abies assembly
5000
10000
15000
20000
5000
10000
15000
20000
D) LTR / LTR−RT Interior ratio
0.2
0.4
0.6
0.8
0.2
0.4
0.6
0.8
B) LTR length (bp)
500
1500
2500
3500
500
1500
2500
3500
E) Identity (%)
84
86
88
90
92
94
96
84
86
88
90
92
94
96
C) Alignment length (bp)
500
1500
2500
3500
500
1500
2500
3500
F) GC (%)
35
40
45
50
55
35
40
45
50
55
LTRs without gene conversion events
LTRs with gene conversion events

Figure 5

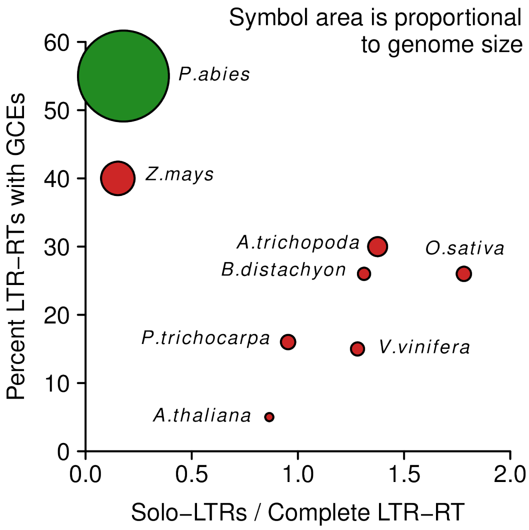
Symbol area is proportional
to genome size
Percent LTR–RTs with GCEs
Solo–LTRs / Complete LTR–RT
0
10
20
30
40
50
60
0.0
0.5
1.0
1.5
2.0
P.abies
Z.mays
A.trichopoda
O.sativa
B.distachyon
P.trichocarpa
V.vinifera
A.thaliana